Accurate Calibration of Low-Speed Wind Tunnels, Including Humidity and Compressibility

Eugene E. Covert* and Frank H. Durgin†
Massachusetts Institute of Technology, Cambridge, Massachusetts 02139

Introduction

IMPROVEMENTS in instrumentation and sensors have the improved measurement accuracy of wind-tunnel data to the 0.1% level. The assumptions and limits underlying the models of the physical processes must be clearly understood to ensure the additional digits in the output are meaningful. Historically, a steady incompressible working fluid has been the model for steady, low-speed flow, and so the relation between dynamic pressure, stagnation pressure, and static pressure is

$$q = \tfrac{1}{2}\rho U_\infty^2 = p_T - p_\infty \tag{1}$$

By convention, the dynamic pressure has been adopted as an aerodynamic reference pressure. Thus the relation between q, the relative velocity V_∞, and Mach number M_∞, and the flow parameters is important. The flow properties include not only total and static pressure, total and static temperature, but also humidity and turbulence level. The following section addresses setting limits for the validity of the assumption of incompressibility during low-speed wind-tunnel testing. The subsequent sections address the correction to humid, unsteady flows.

Compressibility Effects

A gas that is calorically and thermally perfect allows Eq. (1) to be rewritten in the form

$$q = (\gamma/2)p_\infty M_\infty^2 \tag{2}$$

and the square of the Mach number is found from the isentropic pressure-Mach number relation[1]:

$$M_\infty^2 = [2/(\gamma-1)]\left[(p_T/p_\infty)^{(\gamma-1)/\gamma} - 1\right] \tag{3}$$

Here p_T is the stagnation pressure, p_∞ is the static pressure, and γ is the specific heat ratio. To calculate the dynamic pressure based upon the difference between p_T and p_∞, which is usually measured very accurately in low-speed wind tunnels, define

$$p_T/p_\infty = 1 + (p_T - p_\infty)/p_\infty = 1 + \varepsilon \tag{4}$$

Thus Eq. (3) can be written approximately $M_\infty^2 = 2/\gamma \cdot \varepsilon[1 - \varepsilon/2\gamma + o(\varepsilon^2) + \cdots -]$; $o(\varepsilon^2)$ implies term in the series is constant, when divided by ε^2. The term is said to be of the order ε^2 as $\varepsilon \to 0$. Thus

$$q = (p_T - p_\infty)[1 - (1/2\gamma)\varepsilon + o(\varepsilon^2)\cdots] \tag{5}$$

Once the Mach number, the static temperature, and the gas constant R are known, the speed of sound is known, and the wind speed follows by multiplication, i.e.,

$$U_\infty = \sqrt{\gamma R T_\infty} = \sqrt{2RT_T\varepsilon}[1 - 0.45(\varepsilon/\gamma) + o(\varepsilon^2)]M_\infty \tag{6}$$

Shapiro, who solves Eq. (3) for p_T and substitutes into Eq. (1) and expands the bracket, finds

$$(p_T - p_\infty) = q[1 + M^2/4 + o(M^4) + \cdots] \tag{7}$$

In both cases q is function of $p_T - p_\infty$ and a correction term. Thus, if the effect of compressibility on dynamic pressure is to be less than 0.1% the second term in Shapiro's series must be less than 0.001. This implies the Mach number is less than 0.063, or the wind speed is less than roughly 22 m/s.

Correction for Humidity

Customarily the calculations just described are based upon air being a mixture of nitrogen, oxygen, and argon. Thus the value of the gas constant R is 287 $(\text{m/s})^2$ per degree Kelvin.[2] The specific heat ratio in the temperature range of 4 and 32°C may be taken as 1.400 to within 0.04%.

The changes to the gas properties, i.e., the specific heats and the gas constant, are calculated from Dalton's law,[3] which states that gas static pressure is the sum of the partial pressures of the gas's constituents, and from the definition of the specific humidity $\omega = \rho H_2 0/\rho_d$ (Ref. 2), ω as water vapor density divided by the dry air density.

After carrying out the implied calculation, the humidity correction factors can be expressed in terms of ω. Thus if the subscript h denotes humid conditions and the subscript d denotes dry conditions, the density is

$$\rho_h = \rho_d(1 + \omega) \tag{8}$$

ρ_h can also be computed directly (Ref. 4, p. 8; the authors thank Michael Sturgeon of the National Weather Service and a reviewer for this correction procedure). The dry value for the gas constant and the specific heat ratio are corrected for the effects of humidity by multiplying each by a single term. Thus for the gas constant

$$R_h = R_d(1 + 0.609\omega) \tag{9}$$

and for the specific heat ratio

$$\gamma_h = \gamma_d(1 - 0.1\omega) \tag{10}$$

The value of ω can be found using an approximation given next. This requires measurements of relative humidity and static temperature. The saturation pressure is given in Table 1.[2]

If ϕ is the measured relative humidity, then

$$\omega = 0.622\frac{\phi P_{\text{SAT}}}{p_\infty - P_{\text{SAT}}} \tag{11}$$

where p_∞ is the measured static pressure. From Eq. (5)

$$\frac{\partial q}{\partial \omega} = \frac{\partial q}{\partial \gamma}\frac{\partial \gamma}{\partial \omega} = \frac{(p_t - p_\infty)\varepsilon}{\gamma^2(\gamma-1)^2}(-0.1) \tag{12}$$

The combined compressibility and humidity correction is

$$q = \frac{(p_T - p_\infty)\text{meas}}{1 - (\varepsilon/2\gamma)[1 + 0.1\omega/\gamma(\gamma-1)^2]} \tag{13}$$

Because ω is usually less than 3%, the correction term is less than 0.013. In the temperature range of 20°C (68°F) and a relative

Table 1 Saturation pressure of water vapor

Saturated pressure, kPa[a]	Temperature, °C
10	45.8
20	60.1
30	69.1
40	75.9
50	81.4
60	86.0
80	93.5
100	99.6

[a]The saturation vapor pressure can be deduced using the pressure correction term in Eq. (1.19) of Ref. 4.

Received 27 January 2001; revision received 27 August 2001; accepted for publication 29 August 2001.

*T. Wilson Professor Emeritus, Department of Aeronautics and Astronautics. Honorary Fellow AIAA.
†Associate Director, Wright Brothers Wind Tunnel, and Consultant.

humidity of 60%, $\omega = 0.0085$, and so the humidity correction term is 0.0038, which is quite small compared to the compressibility correction term but is large at the 0.1% level.

The corrected value for the velocity is

$$U_\infty = \frac{U_{\text{MEAS}}}{1 - (1 + 0.22/\gamma)\omega} \tag{14}$$

Tunnel Turbulence Level

In the case of randomly fluctuating velocty, the total pressure probe can act to recify the turbulent fluctuation. Thus if u' is a random velocity,

$$p_T = p_\infty + q + \tfrac{1}{2}\rho\overline{u'^2} \tag{15}$$

where

$$\overline{u'^2} = \lim_{t\to\infty} \frac{1}{t}\int_{-t}^{t}\left(\frac{1}{2}\rho\right)u'^2(t)\,\mathrm{d}t$$

and because

$$\lim_{t\to\infty} \frac{1}{t}\int_{-t}^{t}\left(\frac{1}{2}\rho\right)u'(t)\,\mathrm{d}t = 0$$

Thus, the corrected steady flow value is

$$p_T = \frac{p_{T_{\text{meas}}}}{1 + \overline{u'^2}/u_\infty^2} \tag{16}$$

Effects of Condensation; Stagnation Pressure

If the relative humidity level is nearly one, it is possible that a few degrees of cooling in the low-speed wind-tunnel nozzle could lead to condensation of water vapor in the nozzle. For example, an isentropic expansion to $M = 0.10$ reduces the static temperature by about 0.44°C; expansion to $M = 0.3$ reduces the temperature by about 5°C. Depending on the initial humidity level, if there is condensation, the working medium will be a two-phase flow downstream of condensation onset (for a deeper discussion, see Ref. 5).

If all of the water vapor is condensed, the heat released is computed from h_ℓ, the latent heat of condensation. Thus the entropy rise across the condensation region, from state 1 to state 2, is

$$S_2 - S_1 = h_\ell \rho_d \omega / RT \tag{17}$$

For the purpose of this calculation, the saturation temperature is assumed to be the static temperature at the onset of condensation.

The condensation causes a departure from the isentropic condition of less than 0.1% whenever the saturation temperature is less than 24°C.

The effects of condensation appear to be reversable along a stagnation streamline because compression of the gas mixture on that streamline reevaporates the condensed water as the stagnation point is reached. Thus it seems likely that the effect of condensation on the stagnation pressure measurement will be less than the instrument resolution.

Effects of Condensation, Static Pressure

The effect of condensation on static pressure is estimated by Shapiro's one-dimensional flow equation[6] and the assumption that after condensation takes place the water vapor volume goes to zero.

The problem is made more accessible by the fact that the Mach number is small so that the influence coefficients can be given their low-Mach-number limiting forms [i.e., as $(1 - M^2) \to 1$].

The net pressure change results from the temperature rise because the change in mass flux is negligible:

$$\frac{\mathrm{d}p}{p} \cong \gamma M^2\left[-\frac{\mathrm{d}T_t}{T_t}\right] \tag{18}$$

If ω were as large as 3%, the temperature rise would be about 0.42°C. Thus even at $M = 0.4$ the fractional pressure rise is about 0.032% and is thus negligible. Using Eq. (5), it is easy to show the effect of condensation on Mach number squared and on the static and dynamic pressure is neglible in the speed range under discussion. The change in the velocity is of the order of $\sqrt{(\delta T_T/T_T)}$.

Table 2 Examples of the size of the correction of dry air parameters to wet air parameters[a]

Temperature dry bulb, °C	Relative humidity, %	ω	Comment
0	50	0.002	No humidity correction needed at 0.1% level.
20	40	0.006	0.2% correction to velocity; q and M_∞ do not need correction.
20	65	0.010	0.35% correction to velocity −0.1% correction to q; M_∞ does not need correction.
30	90	0.026	0.9% correction to velocity −0.26% correction to q; M_∞ does not need correction.

[a]The measured static and total pressures include the partial pressure of the water vapor. Because the Mach is independent of humidity, the dynamic pressure includes the water vapor. Hence the corrections cause the measured humid air properties to be reduced to dry air values.

Instrument Uncertainties

Modern pressure sensors usually have an accuracy of about 0.1% of full scale. Similarly temperature sensors are capable of measuring a fraction of a degree F, which at room temperatures is also about 0.1%. The rms error in Mach number can be estimated from Eqs. (3) and (5) to be

$$\frac{\delta M_\infty}{M_\infty} = \frac{\gamma - 1}{2\gamma}\frac{1}{1 + (p_T - p_\infty)/p_\infty - [1 + (p_T - p_\infty)/p_\infty]^{1/\gamma}} \times \left[\frac{\delta(p_T - p_\infty)^2}{p_\infty^2} + \left(\frac{p_T - p_\infty}{p_\infty}\right)^2\left(\frac{\delta p_\infty}{p_\infty}\right)^2\right]^{\frac{1}{2}} \tag{19}$$

If the value $(p_T - p_\infty)/p_\infty$ is 0.1 (about 480 km/h) and the transducers have a 0.1% full-scale error, then

$$\frac{\delta M_\infty}{M_\infty} \simeq \frac{1}{2}\frac{\sqrt{2}\times 10^{-3}}{1 + 0.0357 - 0.0015\cdots} \simeq 0.68 \times 10^{-3} \tag{20}$$

which is negligible in most circumstances.

So the error in dynamic pressure and velocity depend upon pressure and temperature transducer error, which is about 0.1% of full scale for pressure and about 0.2 deg for temperature. The error in the relative humidity sensor is of the order of a few percent. The size of ω and its effects on the sensitivities is small enough that the consequences of a few percent error in the relative humidity is neglible.

Generally speaking, the instrument sensivities are of the same order or smaller than the humidity effects. A typical size of the correction to Mach number, dynamic pressure, and velocity is shown in Table 2.

Conclusions

The use of the Mach number and static pressure [Eqs. (2), (3), and (5)] provide an accurate value of dynamic pressure for the whole range of low-speed testing. The use of the isentropic formula for Mach number [Eq. (3)] is effectively independent of humidity. Further the results show that the classical determination of dynamic pressure [Eq. (1)] is in error at the 0.1% level whenever the Mach number exceeds 0.063. The calculation of dry air and steady-state values of velocity and dynamic pressure need a correction dependent upon the specific humidity and turbulence level if these parameters need to be known to the 0.1% level of accuracy.

Acknowledgments

The authors wish to thank J. R. Baron and E. M. Greitzer, as well as the reviewers for their patience and constructive criticism that improved the quality of this material.

References

[1]Liepmann, H. W., and Roshko, A., *Elements of Gas Dynamics*, Guggenheim Aeronautical Series, Wiley, New York, 1957, p. 55 [Eq. (2.40)].

[2]Sherwin, Keith, and Horsley, Michael, *Thermofluids*, Chapman and Hall, New York, 1964, p. 646.
[3]Jeans, Sir James, *Kinetic Theory of Gases*, Cambridge Univ. Press, Cambridge, England, U.K., 1946.
[4]Barlow, Jewel, B., Ray, William, H., Jr., and Pope, Alex, *Low Speed Wind Tunnel Testing*, 3rd ed., Wiley, New York, 1999, p. 222.
[5]Stever, H. Guyford, "Condensation High Speed Flows," Section F, *Fundamentals of Gas Dynamics*, Vol. 3, edited by H. W. Emmons, Princeton Univ. Press, NJ, 1967, pp. 528–572.
[6]Shapiro, Asher, *The Dynamics and Thermodynamics of Compressible Fluid Flow*, Wiley, New York, 1953, pp. 94, 95.

R. P. Lucht
Associate Editor

Full-Field Experimental Investigations on Resonant Vibration of Cracked Rectangular Cantilever Plates

Chien-Ching Ma* and Dong-Ming Hsieh†
National Taiwan University,
Taipei 10617, Taiwan, Republic of China

I. Introduction

ELECTRONIC speckle pattern interferometry (ESPI) was proposed in the 1970s[1] as a method of producing interferograms without using a traditional holographic technique.[2] The main difference between ESPI and holography is the interferometric image processing. The image data are digitized by a video camera and digital signal processor for the ESPI method, which eliminates time-consuming chemical development. Because the interferometric image is recorded and updated by the video camera every $\frac{1}{30}$ s, ESPI is faster in operation and more insensitive to environmental noise than holography. The comparative advantage of operation allows ESPI to extend its application compared with other optical measurement techniques. To increase the visibility of the fringe pattern and to reduce the environmental noise simultaneously, an amplitude-fluctuation ESPI method was proposed by Wang et al.[3] for out-of-plane vibration measurement. In the amplitude-fluctuation (AF) ESPI method, the reference frame is recorded in a vibrating state and subtracted from the incoming frame. Ma and Huang[4] and Huang and Ma[5] used the AF-ESPI method to investigate the three-dimensional vibrations of piezoelectric rectangular parallelepipeds and cylinders; both the resonant frequencies and the mode shapes were presented and discussed in detail.

The study of the vibration behavior of plates with a crack is a problem of great practical interest. Only a few papers have been published on the vibration analysis of a finite cracked plate. This problem combines the fields of vibration analysis and fracture mechanics. If the cracked plate is in resonance, the crack can propagate either explosively or faster than in the early stage. To avoid the mentioned fracture produced by vibration, it is necessary that the vibration characteristics of the cracked cantilever plate be clarified. Nevertheless, compared with studies in the past, there is little research on the influence of cracks on the vibration behavior of plates.

In this Note, we employ an optical method based on the AF-ESPI to study the resonant properties of rectangular cantilever plates with cracks. The rectangular cantilever plate is clamped along one edge and free along the other three edges; a straight crack is located along the clamped edge. The advantage of using the AF-ESPI method is that resonant frequencies and the corresponding mode shapes can be obtained simultaneously from the experimental measurement. In addition to the AF-ESPI method, numerical computations based on a finite element package are presented, and good agreement is found in comparison with experimental results for both the resonant frequency and vibration mode shapes. The quantitative magnitudes of the full field vibration displacements are also indicated in the experimental results, which are in the order of a micrometer.

Received 18 July 2000; revision received 20 April 2001; accepted for publication 4 June 2001.

*Professor, Department of Mechanical Engineering; cma@w3.me.ntu.edu.tw.
†Graduate Student, Department of Mechanical Engineering.

II. Experimental Measurements and Numerical Results

The optical arrangement for out-of-plane vibrating measurement by ESPI is shown schematically in Fig. 1. If the image is taken after the specimen vibrates periodically, the light intensity detected by a charge-coupled device (CCD) camera is indicated as I_1. The AF-ESPI method is employed in this study by taking two images while the specimen vibrates and assuming that the vibration amplitude of the second image has changed from A to $A + \Delta A$ due to the unstability of apparatus. The light intensity of the second image is indicated as I_2. When these two images (I_1 and I_2) are subtracted and rectified by the image processing system, the resulting image intensity can be expressed as[4]

$$I = I_2 - I_1 = \sqrt{I_A I_B}/2\left|(\cos\phi)\Gamma^2(\Delta A)^2 J_0(\Gamma A)\right| \qquad (1)$$

where I_A is the object light intensity, I_B is the reference light intensity, ϕ is the phase difference between object and reference light, J_0

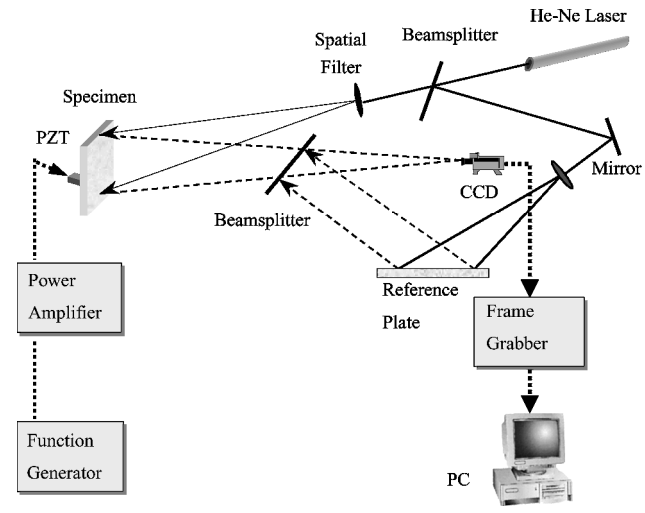

Fig. 1 Schematic diagram of ESPI experimental setup for out-of-plane measurement.

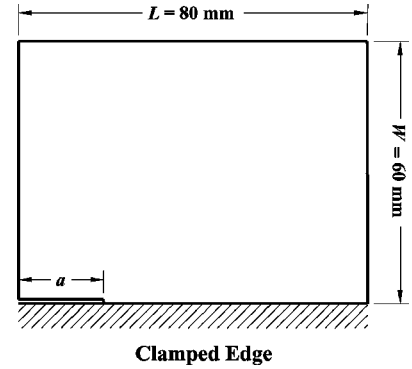

Fig. 2 Geometric dimensions and configuration of cracked rectangular plates: thickness h = 1 mm and crack length a = 20, 35, and 50 mm.